

Ultra-Compact Dual-Band 3-D Hilbert Resonator in LTCC Technology

Nikolina Janković, Vasa Radonić and Vesna Crnojević-Bengin

University of Novi Sad, Faculty of Technical Sciences, Novi Sad, Serbia

Abstract: An ultra-compact dual-band resonator is presented based on a three-dimensional Hilbert fractal curve, with the overall dimensions equal to only $\lambda_g/25 \times \lambda_g/25 \times \lambda_g/25$, where λ_g denotes the guided wavelength at the first resonant frequency. Although in essence being a conventional half-wavelength resonator, 3-D Hilbert resonator can also be used as a dual-band resonator since its first and second harmonic resonances can be independently controlled due to its multilayer geometry. The resonator has been fabricated in Low Temperature Co-fired Ceramics (LTCC) technology using DuPont 951 Green Tape and a very good agreement between the simulated and measured responses has been obtained, proving LTCC to be very suitable for the fabrication of multilayer microwave passive devices.

Keywords: microwave resonator, fractal curve, multilayer structure, LTCC, dual-band filter

Ultra kompakten dvopasovni resonator v LTCC tehnologiji

Izveček: Predstavljen je ultra kompakten dvopasovni resonator, ki temelji na tridimenzionalni Hilbertovi fraktalni krivulji. Velikosti so le $\lambda_g/25 \times \lambda_g/25 \times \lambda_g/25$, kjer λ_g predstavlja vodilno valovno dolžino pri prvi resonančni frekvenci. Čeprav je 3D Hilbertov resonator v osnovi klasičen pol-valoven resonator se ga, zaradi večplastne strukture in možnosti ločenega kontroliranja druge in tretje harmonične frekvence, uporablja kot dvopasovni resonator. Resonator je bil izdelan v tehnologiji DuPont 951 Green Tape nizkotemperaturne sočasno sintrane keramike (LTCC). Dobra ujemanja rezultatov simulacij z meritvami potrjujejo uporabnost LTCC postopka za izdelavo večslojnih mikrovalovnih pasivnih elementov.

Ključne besede: mikrovalovni resonator, fraktalne krivulje, večslojna struktura, LTCC, dvopasovni filter

* Corresponding Author's e-mail: nikolina@uns.ac.rs

1. Introduction

Due to the rapid development of various wireless communication systems, there is an ever-increasing demand for low-cost, high-performance and compact microwave devices such as filters and their building blocks - resonators. The most common approach to miniaturisation of microwave resonators is based on folding the conventional straight-line resonator in order to fit it in a smaller area. However, this also reduces performances of the resonator and the final filter.

Recently, deployment of fractal curves has been suggested as the most prominent way to reduce the size of a resonator, while preserving its performance, [1]. Due to their unique space-filling property, fractal curves theoretically allow the design of infinite-length lines on a finite substrate area. Different fractal geometries, most often Hilbert and Peano fractals, have been uti-

lized in the design of miniaturized antennas [2-7], high impedance surfaces, [8-9], left-handed metamaterials, [10], RFID tags, [11], and filters, [12-15]. In [16] we have shown that a planar resonator based on two-dimensional (2-D) Hilbert fractal curve is superior to all other non-fractal configurations, both in terms of the circuit size as well as in terms of the quality factor.

Resonators based on the three-dimensional (3-D) Hilbert fractal curve and several other multilayer geometries have been analysed and compared in [17]. 3-D Hilbert resonator has been proven to be superior to its 2-D counterparts as well as to other 3-D geometries.

On the other hand, beside compact size modern wireless systems also demand passive devices that simultaneously operate at two or more arbitrary (non-harmonically related) frequencies. This cannot be easily achieved by using conventional half-wavelength or

quarter-wavelength resonators since their harmonics cannot be independently controlled. In this paper, we show that 3-D Hilbert resonator can be used as a dual-band resonator, with arbitrarily positioned operating frequencies. Namely, mutual coupling between the adjacent conductive layers strongly affects the response of the resonator and the positions of the first and second resonant frequency can be almost independently controlled by proper variation of certain geometrical parameters.

The optimized resonator has been fabricated in Low Temperature Co-fired Ceramics (LTCC) technology. LTCC originates from microelectronics but is more and more used today in microwave engineering, since it involves single-step lamination and firing which makes it very reliable and particularly advantageous for fabrication of complex structures with many conductive layers.

2. Configuration and Results

Fractal curves are generated in an iterative manner by successive repetition of one geometrical shape with the other (that often is a collection of scaled copies of the first shape). After each iteration a fractal curve of the higher order is obtained, longer than the previous one, which better fills the space in which it is generated. This space-filling property of fractal curves offers high potentials for miniaturization of passive microwave circuits because, theoretically, the application of fractal curves allows the design of infinite-length lines on a finite substrate area. Fractal curves are characterized by the fractal (i.e. non-integer) dimension. The dimension of every fractal curve is a number between 1 and 2, and can be understood as a measure of the space-filling ability of the fractal curve. The higher the fractal dimension, the better the fractal curve fills the given area, therefore achieving higher compactness. Only a fractal curve with the maximal possible fractal dimension will after infinite number of iterations entirely fill the rectangular space in which it is designed. Three 2-D fractal curves are known that have maximal fractal dimension: square Sierpinski, Peano, and Hilbert fractals [18]. Unlike Peano and Hilbert, Square Sierpinski fractal has ends on the same side of the line, thus being unsuitable for the design of end-coupled microstrip resonators. Due to the specific shape of the line, Hilbert resonator exhibits larger inductance and therefore larger miniaturization potential than its Peano counterpart, and that is why Hilbert fractal has been chosen as the basis for this work.

3-D Hilbert fractal line can be designed analogously to its 2-D counterpart. In Fig. 1, 3-D Hilbert fractal curve

of the third order is shown that is used for the design of the 3-D Hilbert resonator. The proposed fractal resonator, shown in Fig. 2, consists of four conductive and five dielectric layers, placed over the common ground. DuPont 951 Green Tape has been used with dielectric constant and loss tangent of $\epsilon_r=7.8$ and 0.006, respectively. The thickness of each dielectric layer is initially chosen to be $H=400 \mu\text{m}$. The resonator is made of the conductive line whose width w and spacing g are equal in all layers, $w=g=200 \mu\text{m}$. Adjacent conductive layers are connected by vias whose diameters are equal to the width of the lines to achieve impedance matching. The resonator is capacitively coupled to 50Ω feed lines by using $50 \mu\text{m}$ gaps. The feed lines are positioned on the top (fourth) conductive layer. The role of the top dielectric layer is to provide that the conductive lines in the fourth layer have approximately the same characteristic impedance as those in the lower layers.

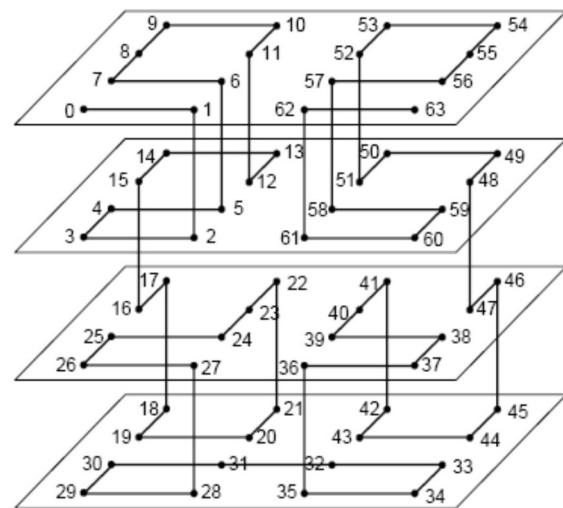


Figure 1: Schematic view of 3-D Hilbert fractal curve of the third order. The line starts at the node denoted with 0 and ends at the node denoted with 63.

Simulated response of the proposed resonator is shown in Fig. 3. The simulations have been carried out using Ansoft HFSS full-wave simulator. From the positions of maximums of H-field at the first and second resonant frequency, it is evident that the resonator behaves as a conventional half-wavelength resonator. The first resonance occurs at 3.32 GHz which corresponds well to the theoretical half-wavelength resonance on a given substrate, taking into account the mutual inductance between the adjacent layers that reduces the total inductance of the 3-D Hilbert resonator. The first resonance is characterized by high selectivity and low insertion loss of 1.85 dB. As expected, the second harmonic occurs at 7.23 GHz, i.e. at approximately twice the frequency of the fundamental resonance. It is also characterized by low insertion loss of 1.21 dB.

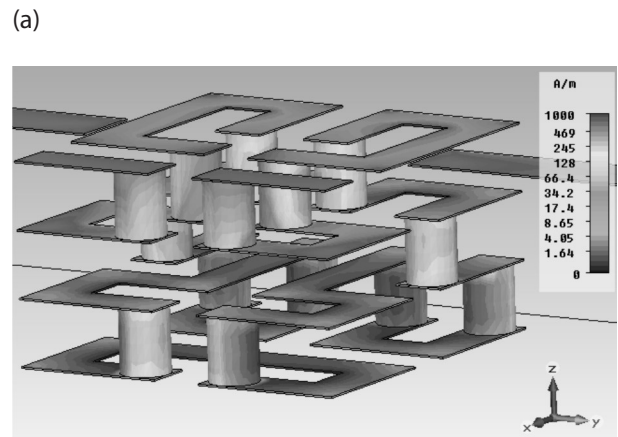
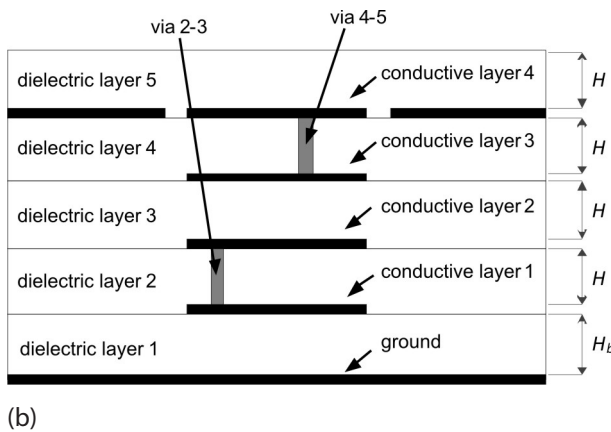
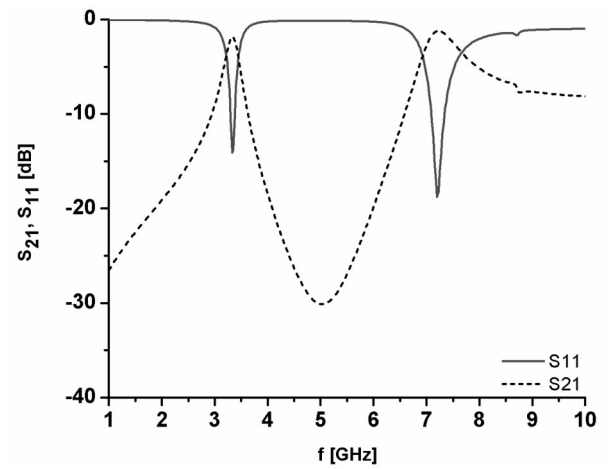
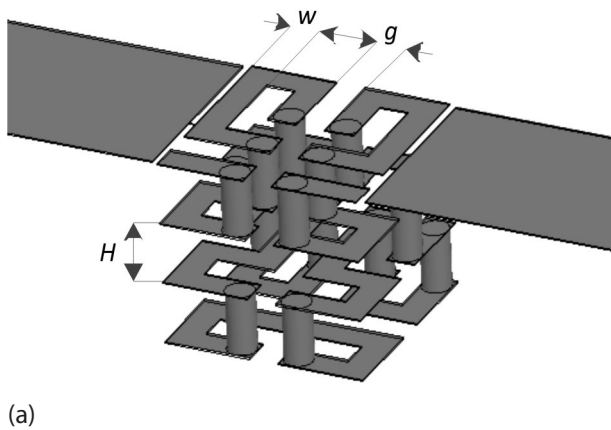


Figure 2: (a) 3-D Hilbert resonator. (b) Cross sectional view of the 3-D Hilbert resonator.

3. Influence of Different Geometrical Parameters on 3-D Hilbert Performances

In order to investigate influence of different geometrical parameters on the performance of the proposed resonator, firstly the fractal resonator line width and spacing have been simultaneously varied between $w=g=200\ \mu\text{m}$ and $w=g=350\ \mu\text{m}$, Fig. 4. As expected, both resonant frequencies are lowered as w and g are increased, due to changed inductance and capacitance of the resonator. At the same time, insertion losses are increased and the selectivity of the passbands is improved.

Dielectric layers in LTCC technology are made up of a number of Green tape layers. Therefore, they can have almost arbitrary overall thickness. We have investigated the influence of dielectric layer thickness on performance of 3-D Hilbert resonator by simultaneously varying thickness of all dielectric layers from $H=100\ \mu\text{m}$ to $H=400\ \mu\text{m}$. Fractal line width and spacing were

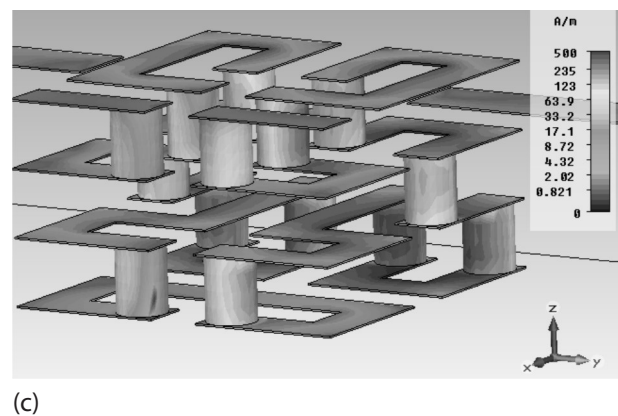


Figure 3: Simulated response of the 3-D Hilbert resonator: (a) Scattering parameters, (b) H-field at the first resonant frequency, (c) H-field at the second resonant frequency.

kept equal to $200\ \mu\text{m}$ in all cases, Fig. 5. Decreasing H enhances mutual coupling between the adjacent layers. Since maximums of E and H fields at the first and second resonance are located on different conductive layers of 3-D Hilbert, Fig. 3 (b) and (c), they are differently affected by changing the dielectric layer thickness: when H is decreased, the first resonance is shifted

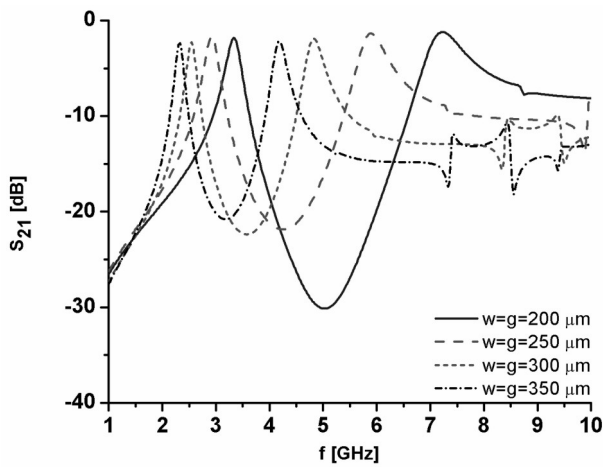


Figure 4: Influence of the line width w and spacing g of the 3-D Hilbert resonator on its performance.

towards higher frequencies while the second harmonic remains almost unaffected. Although decrease in layer thickness degrades the insertion losses, it represents a mechanism that can be used to change the position of the first resonance and, at the same time, keep the second harmonic unaffected, thus opening up possibilities to use 3-D Hilbert resonator as a dual-band resonator with independently positioned passbands.

It is also interesting to note how a change in the thickness of the bottom dielectric layer only, denoted with H_b in Fig. 2(b), affects the response of the resonator. A configuration with thickness of all dielectric layers equal to $H=H_b=400 \mu\text{m}$ has been compared to the one where the thickness of the lowest dielectric layer is reduced to $H_b=100 \mu\text{m}$. Decreasing H_b increases the capacitance between the resonator and the ground. The maximum of E field is located in the top conductive layer in the case of the first resonance, and in the bottom conductive layer in the case of the second resonance. Therefore, only the second resonance is significantly affected by changing H_b which results in a shift of the second harmonic towards lower frequencies, Fig. 6, while the first resonance remains unchanged. This presents additional mechanism for independent control of positions of the two passbands of 3-D Hilbert dual-band resonator.

It can be concluded that changing the layer thickness, i.e. changing the mutual coupling between the layers is the key mechanism to vary relative position of the first and second resonance, i.e. to independently control the positions of the passbands. Therefore, 3-D Hilbert resonator can be used as a dual-band resonator, where relative position of two resonances can be changed in the range from 1.29 to 2.18, as seen in Fig. 5 and Fig. 6.

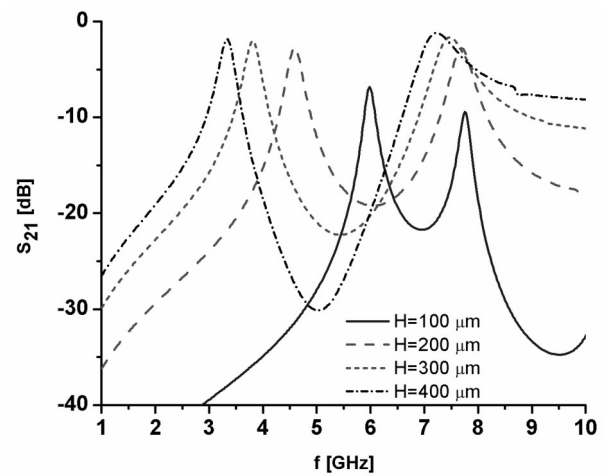


Figure 5: Influence of the thickness of the dielectric layers H on the performance of 3-D Hilbert resonator. Thickness of all dielectric layers H is varied simultaneously. Fractal line width and spacing are equal to 200 μm in all cases.

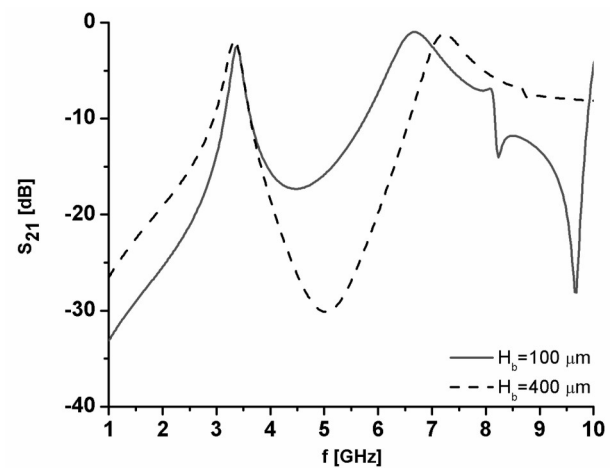


Figure 6: Influence of the thickness of the bottom dielectric layer, H_b . All upper dielectric layers are $H=400 \mu\text{m}$ thick. Fractal line width and spacing are equal to 200 μm .

4. Fabrication and Measurement Results

Analysis presented above also reveals that various optimisation goals used in the design of dual-band 3-D Hilbert resonator, namely minimisation of insertion losses at both resonances, maximisation of the attenuation in the stop band and selectivity of the passbands, are contradictory and thus a trade-off is needed. The configuration with $H=H_b=400 \mu\text{m}$ and $w=g=300 \mu\text{m}$ offers the best trade-off and it has been selected for fabrication. The first and second resonances are positioned

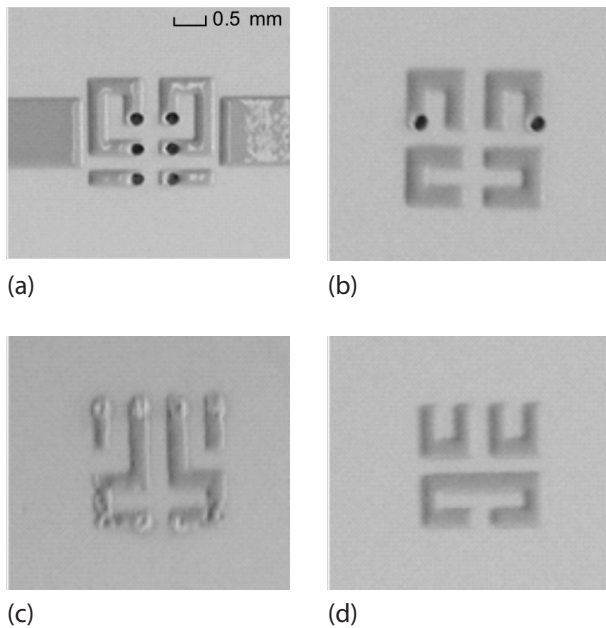


Figure 7: Photographs of the conductive layers of the resonator after conductor printing: (a) conductive layer 4 (top), (b) conductive layer 3, (c) conductive layer 2, (d) conductive layer 1 (bottom).

at 2.55 GHz and 4.83 GHz and corresponding insertion losses are -2.28 dB and -1.88 dB, respectively. The overall dimensions of the resonator are ultra-compact: They are equal to only $2.1 \times 2.1 \times 2$ mm³ i.e. $\lambda_g/25 \times \lambda_g/25 \times \lambda_g/25$, where λ_g is the guided wavelength.

To validate the simulation results, the optimised 3-D Hilbert resonator has been fabricated in LTCC technology. Since the minimum available spacing between two lines in the fabrication process available to us was 120 μ m, the resonator with 120 μ m gaps to the feed lines has been fabricated, instead of 50 μ m used in simulations to characterize the resonator. This change is not crucial, since it practically influences only the insertion losses. Furthermore, it should be noted that gaps of 50 μ m are achievable in standard LTCC technology by using screens with higher resolution or by laser trimming.

Standard LTCC procedure that includes several well-known steps was used. DuPont 951 Green Tape has been used for the fabrication of dielectric layers, with thickness equal to 114 μ m. Since dielectric layers of the resonator should be 400 μ m thick, and since shrinking of approximately 14% was specified, four green tapes have been used for each layer.

After preconditioning of the tapes, via holes were patterned and filled, and conductors in all four conductive layers were printed. For via filling and printing of the conductive layers, DuPont 6141 and 6142D silver pastes compatible with Green tape have been used.

Since the via diameter is equal to the line width, a great degree of precision during the process of via processing was required. Also, considerable attention was paid to via filling to ensure a good connection between adjacent conductive layers. Fig. 7 shows photographs of the conductive layers of the resonator after conductor printing. It can be seen that all lines and spacings have been accurately reproduced, using standard LTCC procedure and with no laser trimming. This proves the potential of LTCC technology for fabrication of compact microwave passive devices. Fig. 8 shows microscopic view of the filled via holes that connect the third and fourth conductive layer. All vias were filled entirely, resulting in minimized losses observed in the measured response.

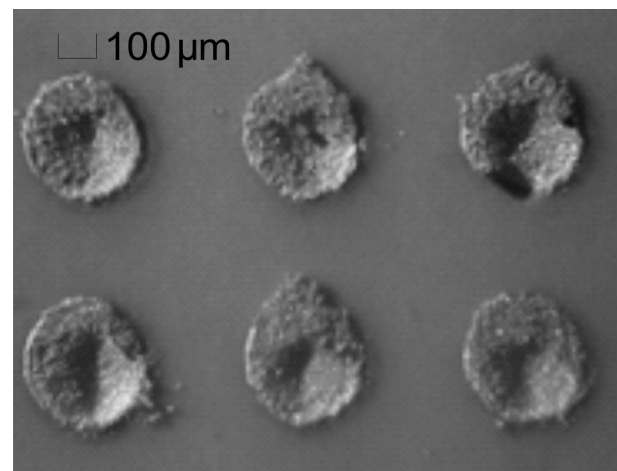


Figure 8: Microscopic view of the filled via holes that connect the third and fourth conductive layers.

In lamination process all layers were stacked together, placed in a vacuum sealed package, and pressed in water in an isostatic press at around 70°C and 3 MPa during 5 minutes. Afterwards, the laminated circuit has been fired in the furnace according to a firing profile given by the manufacturer [19]. After firing and shrinkage of the green tapes, the desired thickness of the layers has been achieved.

In order to enable soldering of connectors to the fabricated circuit, 3 mm x 3.5 mm slits in the top dielectric layer above the feed lines have been made. A special attention was paid to soldering the connectors: it was performed on a pre-heated circuit to avoid defects which might occur due to non-uniform heating of the structure.

Comparison of simulated and measured responses reveals a very good agreement, Fig. 9. The fabricated dual-band 3-D Hilbert resonator exhibits insertion losses of 3.7 dB and 3.8 dB at 2.63 GHz and 5.09 GHz, respectively, while the attenuation between the passbands is more than 27 dB. Fractional bandwidths are 6.8% and

5.3%, respectively. The obtained measurement results also prove that LTCC technology can straightforwardly be used for fabrication of ultra-compact microwave multilayer structures.

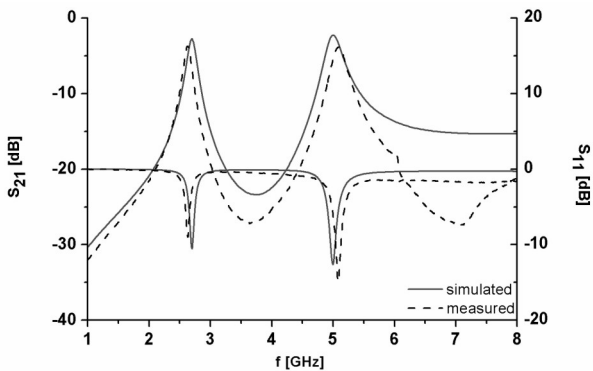


Figure 9: Simulated (red fullline) and measured (black dashed line) responses of the 3-D Hilbert resonator in LTCC technology.

5. Conclusion

In this paper, an ultra-compact dual-band multilayer microstrip resonator with overall dimensions equal to $\lambda_g/25 \times \lambda_g/25 \times \lambda_g/25$ based on 3-D Hilbert fractal curve has been proposed. The influence of different geometrical parameters to its performances has been analysed in detail.

Although the resonator is basically a conventional half-wavelength resonator, it has been shown that it can be used as a dual-band resonator that operates at arbitrary (non-harmonic) frequencies, due to the fact that its multilayer configuration provides a mechanism for independent control of the first and second resonance.

The resonator that offers the best trade-off between the insertion losses, attenuation and selectivity has been designed to operate at 2.55 GHz and 4.83 GHz with insertion losses of -2.28 dB and -1.88 dB, respectively. The resonator has been fabricated in LTCC technology using DuPont 951 Green Tape. The simulated and measured responses agree very well, proving the potential of LTCC technology for fabrication of ultra-compact multilayer microwave passive devices.

Acknowledgement

The authors thank Prof. George Goussetis and Yves Lacrotte from Heriot-Watt University, United Kingdom, for their help with fabrication of the circuit in LTCC technology.

References

1. P. Jarry and J. Beneat, Design and realization of miniaturized fractal RF and microwave filters. New Jersey, John Wiley, 2009.
2. K.J. Vinoy, K.A. Jose, V.K. Varadan, and V.V. Varadan, "Hilbert curve fractal antenna: A small resonant antenna for VHF/UHF applications," Microwave and Optical Technology Letters, vol. 29, pp. 215–219, 2001.
3. J. Anguera, C. Puente, E. Martínez, and E. Rozan, "The fractal Hilbert monopole: A two-dimensional wire," Microwave and Optical Technology Letters, vol. 36, pp. 102–104, 2003.
4. J. Zhu, A. Hoorfar, and N. Engheta, "Bandwidth, cross-polarization, and feed-point characteristics of matched Hilbert antennas," IEEE Antennas Wireless Propagation Letters, vol. 2, pp. 2–5, 2003.
5. J. Zhu, A. Hoorfar, and N. Engheta, "Peano antennas," IEEE Antennas Wireless Propagation Letters, vol. 3, pp. 71–74, 2004.
6. W. Chen, G. Wang, C. Zhang, "Small-size microstrip patch antennas combining Koch and Sierpinski fractal shapes," Antennas and Wireless Propagation Letters, vol. 7, pp. 738–741, July 2008.
7. L. Yousefi, O.M. Ramahi, "Miniaturised antennas using artificial magnetic materials," Electronics Letters, vol. 46, pp. 816–817, June 2010.
8. J. McVay, N. Engheta, and A. Hoorfar, "High-impedance metamaterial surfaces using Hilbert-curve inclusions," IEEE Microwave and Wireless Components Letters, vol. 14, no. 3, pp. 130–132, March 2004.
9. J. McVay, A. Hoorfar, and N. Engheta, "Peano high-impedance surfaces," Radio Sci, 40, RS6S03, 2005.
10. J. McVay, N. Engheta, and A. Hoorfar, "Numerical study and parameter estimation for double-negative metamaterials with Hilbert-curve inclusions," Proceedings of 2005 IEEE Antennas Propagation Society International Symposium, Washington, DC, vol. 2B, pp. 328–331, July 2005.
11. J. McVay, A. Hoorfar, and N. Engheta, "Space-filling curve RFID tags," Proceedings of IEEE Radio and Wireless Symposium, San Diego, CA, pp. 199–202, January 2006.
12. N. Janković, V. Radonić and V. Crnojević-Bengin, "Novel bandpass filters based on grounded Hilbert fractal resonators," 3rd International Congress on Advanced Electromagnetic Materials in Microwaves and Optics, London, UK, August 2009.
13. W. Chen, G. Wang, "Effective design of novel compact fractal-shaped microstrip coupled line bandpass filters for suppression of the second harmonic," Microwave and Wireless Component Letters, vol. 19, pp. 74–76, February 2009.

14. D. Oloumi, A. Kordzadeh, A. Neyestanak, "Size reduction and bandwidth enhancement of a waveguide bandpass filter using fractal-shaped irises," *Antennas and Wireless Propagation Letters*, vol. 8, pp. 1214-1217, October 2009.
15. H. Xu, G. Wang, C. Zhang, "Fractal-shaped UWB bandpass filter based on composite right/left handed transmission line," *Electronics Letters*, vol. 46, pp. 285-287, February 2010.
16. V. Crnojević-Bengin, "Novel compact microstrip resonators with multiple 2-D Hilbert fractal curves," *Microwave and Optical Technology Letters*, vol. 48, no.2, pp.270-273, February 2006.
17. V. Crnojević-Bengin and Đ. Budimir, "Novel 3-D Hilbert microstrip resonators," *Microwave and Optical Technology Letters*, vol. 46, no. 3, pp. 195-197, August 2005.
18. V. Crnojević-Bengin, V. Radonić and B. Jakanović, "Fractal Geometries of Complementary Split-Ring Resonators," *IEEE Trans. Microw. Theory Tech.*, vol. 56, no. 10, pp. 2312- 2321, Oct. 2008.
19. http://www2.dupont.com/MCM/en_US/assets/downloads/prodinfo/951LTCCGreenTape.pdf

Arrived: 16. 08. 2012

Accepted: 12. 11. 2012